International Journal of General Medicine

Dovepress
Taylor & Francis Group

Open Access Full Text Article

ORIGINAL RESEARCH

Identification of Pivotal ceRNA Networks Associated with Stanford-A Aortic Dissection via Integrated Bioinformatics Analysis

Yuyuan Hu[1,*], Zhenhao Liu[2,*], Yan Qin[3,*], Nan Wu[4], Tao Yang[2], Xinmeng Cheng[5], Chunyan Wang[6], Xuening Wang[2]

[1]Department of Cardiac Surgery, the First Affiliated Hospital of Shandong Second Medical University, Weifang, 261000, People's Republic of China; [2]Third Hospital of Shanxi Medical University, Shanxi Bethune Hospital, Shanxi Academy of Medical Sciences Tongji Shanxi Hospital, Taiyuan, 030032, People's Republic of China; [3]Department of Science and Technology Education, Shanxi Center for Clinical Laboratory, Taiyuan, 030012, People's Republic of China; [4]Department of Cardiac Surgery, Shanxi Provincial People's Hospital, Fifth Hospital of Shanxi Medical University, Taiyuan, 030012, People's Republic of China; [5]Department of Cardiovascular Surgery, the Affiliated Cardiovascular Hospital of Shanxi Medical University and Shanxi Cardiovascular Hospital (Institute), Taiyuan, Shanxi, 030000, People's Republic of China; [6]Department of Clinical Laboratory, Shanxi Province Cancer Hospital, Shanxi Hospital Affiliated to Cancer Hospital, Chinese Academy of Medical Sciences, Cancer Hospital Affiliated to Shanxi Medical University, Taiyuan, 030013, People's Republic of China

*These authors contributed equally to this work

Correspondence: Xuening Wang, Department of Cardiovascular Surgery, Third Hospital of Shanxi Medical University, Shanxi Bethune Hospital, Shanxi Academy of Medical Sciences, Tongji Shanxi Hospital, 99 Longcheng Road, Taiyuan, 030032, People's Republic of China, Tel +86 15035118416, Email wangxuening2004@126.com; Chunyan Wang, Shanxi Province Cancer Hospital/ Shanxi Hospital Affiliated to Cancer Hospital, Chinese Academy of Medical Sciences/Cancer Hospital Affiliated to Shanxi Medical University, No. 3 Zhigongxin Street, Xinghualing, Taiyuan, Shanxi, People's Republic of China, +86 15110313926, Email chunyanwang2007@163.com

Objective: Stanford-A Aortic dissection (TAAD) is a rare and fatal disease, genetic factors remains poorly known. Study has confirmed that lncRNA play an important role in various physiological and pathological processes. This study attempts to elucidate the underlying molecular mechanisms of TAAD through lncRNA-associated competitive endogenous RNA (ceRNA) networks.

Methods: In this study, aortic vascular of 5 TAAD and 5 control (ischemic heart disease) were subjected to lncRNA and mRNA microarray analysis, and differentially expressed mRNAs (DEGs) and differentially expressed lncRNAs (DELs) were identified. The differentially expressed miRNAs (DEmiR) were screened by GSE98770 dataset. The ceRNA network (lncRNA-miRNA-mRNA) was constructed by bioinformatics analysis. The accuracy of hub genes as biomarkers for predicting TAAD was evaluated by receiver operating characteristic (ROC) curve. Finally, the biomarkers were verified by assessing their mRNA levels using real-time quantitative PCR (RT-qPCR).

Results: This study revealed 161 DELs, 87 DEmiRs and 103 DEGs between TAAD and control. We constructed ceRNA networks based on the screened 1 lncRNA, 4 miRNAs and 7 mRNAs. We identified three lncRNA-miRNA-mRNA regulatory axes, namely the VCAN axis (LINC01355 - hsa-miR-186-5p / hsa-miR-30a-5p /hsa-miR-30c-5p - VCAN), LOX axis (LINC01355-hsa-miR-145-5p/ hsa-miR-186-5p/ hsa-miR-30a-5p / hsa-miR-30c-5p - LOX), and CTSS axis (LINC01355 - hsa-miR-186-5p - CTSS) based on gene ontology, pathway enrichment and protein-protein interaction (PPI) network, which may play an important role in TAAD. The clinical performance of VCAN, CTSS, and LOX in TAAD diagnosis was evaluated, and the AUCs of VCAN, CTSS, and LOX were 0.920 ($p<0.001$), 0.880 ($p=0.002$) and 0.840 ($p=0.011$), respectively. Furthermore, mRNA expression of VCAN in human aortic tissue significantly overexpressed in the TAAD patients ($p<0.001$).

Conclusion: This study identifies three ceRNA interaction axes, especially VCAN associated with TAAD pathogenesis, providing fundamentals of bioinformatics for understanding the molecular mechanisms of TAAD pathogenesis and developing potential therapeutic strategies for TAAD.

Keywords: Stanford-A aortic dissection, lncRNA, ceRNA network, VCAN, bioinformatics analysis

Received: 28 November 2024
Accepted: 28 February 2025
Published: 17 March 2025

Introduction

Stanford-A aortic dissection (TAAD) is a serious aortic disease, which is characterized by the separation of thoracic aortic medial layers.[1] At present, the surgical treatment of TAAD is complicated, and it is not effective in controlling the bleeding of patients.[2] During open surgery, patients may experience many complications, with high mortality rates worldwide.[3] Therefore, it is urgent to search favorable therapeutic targets to prevent the pathologic development of TAAD.

The development of microarray analysis and modern bioinformatics technology has made it possible to study the genetics of TAAD. Recent years, high-throughput sequencing (HTS) technology has be used to characterize the genetic basis of diseases due to its ability to analyze the whole transcriptome. Currently, HTS research focuses on identifying differentially expressed genes (DEGs), however, the key genes that cause TAAD have yet to been discovered.[4,5]

Long non-coding RNA (lncRNA) are defined as more than 200 nucleotides in length and found to regulate protein coding gene expression at both the transcriptional and post transcriptional levels.[6] Moreover, study has observed that, as the new epigenetic regulatory molecules, lncRNA can alter the expression degree and biological function of miRNA as an endogenous sponge in the pathophysiology of blood vessels.[7–9] Current few studies involve lncRNA expression profiles in TAAD tissues, especially in human TAAD tissues.

This study focused on the bioinformatics analysis of HTS, and construct the lncRNA expression profile and ceRNA network of TAAD. By combining bioinformatics tools, such as R software with Gene Expression Omnibus 2R analysis, target gene prediction tools, gene ontology (GO) and pathway analysis, and protein-protein interaction (PPI) networks, we identified specific lncRNAs and ceRNA interaction axes closely related to the pathogenesis of TAAD.

Materials and Methods

Sample Collection

A total of 5 TAAD and 5 control (ischemic heart disease) at the Shanxi Bethune Hospital between June 2020 and October 2020 were included in this study. Patients who were younger than 18 years of age or pregnant, or who suffered from a malignant disease (a cancer/tumor), an infection, hypertension, diabetes mellitus, aortic atherosclerotic plaque or calcification, and abnormal levels of myocardial enzymes, troponin, and neutrophils, or other cardiovascular diseases, were excluded. During surgery, small segments of human ascending aorta samples were taken from patients who had ischemic heart disease. These samples were collected under strict sterile conditions immediately after aortic cannulation or partial clamping, following standardized protocols to ensure the integrity and quality of the tissue samples. This study was conducted in accordance with the Declaration of Helsinki and was approved by the Shanxi Bethune Hospital (IRB: SBQKL-2022-034). Before deciding to take part in this trial, written informed consent was obtained from every patient.

Microarray Data Acquisition

RNA was extracted from aortic tissue of 5 TAAD patients and 5 control (ischemic heart disease) by Trizol and organic solvents (Invitrogen, CA, USA). The NanoDrop ND-1000 (IMPLEN,CA,USA) was used to measure the quantity and quality of RNA. RNA integrity was evaluated using the Agilent 2100 Bioanalyzer or customary denaturing agarose gel electrophoresis. The Arraystar Human LncRNA Microarray V5.0 is intended for the worldwide profiling of protein-coding transcripts and human lncRNAs. The Agilent One-Color Microarray-Based Gene Expression Analysis technique were used to sample labeling and array hybridization.

Microarray Data Analysis

Agilent Feature Extraction software (v11.0.1.1) was used to obtain microarray profiles and raw reads. Raw data were normalized with the use of GeneSpring GX v12.1 software (Agilent Technologies). Following normalization of the raw data, lncRNAs and mRNAs with Present or Marginal ("All Targets Value") in at least five out of ten samples were chosen for additional data analysis. P-value and FDR filtering were used to find differentially expressed lncRNAs (DElncRNA) and mRNAs (DEmRNA) between the TAAD and control groups.

Differentially Expressed miRNAs (DEmiRs) Analysis

The National Center for Biotechnology Information's (NCBI) GEO database was searched, and a dataset was acquired by changing the screening criteria for species type to "Homo sapiens". The "expression profiling by array" and "aortic dissection" as the learning type to get a standardized miRNAs expression profiles. Gene Expression Omnibus 2R was used to obtain up and down DEmiRs, the selection criteria was |log2 (fold change)|>1 and p-value ≤ 0.05.

Gene Ontology (GO) and Kyoto Encyclopedia of Genes and Genomes (KEGG) Analysis

GO enrichment and KEGG pathway analyses were provided by online bioinformatics database DAVID (the Database for Annotation, Visualization, and Integrated Discovery) in this study.[10] Cellular component (CC), biological process (BP), and molecular function (MF) were provided in the GO analysis. KEGG was used to explore the pathway enrichment of differentially expressed gene, and gene number >2 and p ≤ 0.05 were set as cut-off points.

Protein–Protein Interaction (PPI) Network Analysis and Key Gene Identification

On the basis of differentially expressed gene, the Search Tool for the Retrieval of Interacting Genes/Proteins (STRING; version 11.0) was used to obtain protein–protein interaction (PPI). After hiding the points without interaction, the data were imported into Cytoscape (version 3.7.2) to visualize the PPI network. The top 10 hub genes in the PPI network were identified using the CytoHubba. GeneMANIA (https://genemania.org) analysis was used to analyze the enrichment of the top 10 hub genes in cellular components and linked pathways.

Prediction of Targeting Relationship and Construction of ceRNA Networks

The top 10 central genes (RNASEL, CTSL, LOX, CTSS, VCAN, PLOD2, IFITM2, CTSH, AMFR, ZNRF4) were selected and miRNA was predicted using TargetScan (www.targetscan.org). The differentially expressed miRNAs in microarray data and predicted miRNAs from the gene map were imported into the functional enrichment analysis website (Draw Venn Diagram (ugent.be)) to take the intersection, and a list of differentially expressed miRNAs were obtain. Furthermore, the relevant lncRNAs were predicted by ENCORI (Encyclopedia of RNA interactomes. (sysu.edu.cn)) Similarly, the differentially expressed lncRNAs in microarray data and predicted lncRNAs were performed the functional enrichment analysis (Draw Venn Diagram (ugent.be)) to take the intersection. Finally, according to the ceRNAs theory, the predicted targets of up-regulated lncRNAs, down-regulated miRNAs, and up-regulated mRNAs were overlapped to construct and visualize ceRNA network (lncRNA-miRNAs-mRNAs) by Cytoscape software.

Real-Time Quantitative PCR (RT-qPCR)

Total RNA was extracted from 100 mg human aortic tissue by real-time quantitative PCR (RT-qPCR) using TRIzol kit at 4°C according to the manufacturer's instructions. Then, the extracted RNA was reverse transcribed into cDNA using a cDNA Synthesis Kit. β-Actin was used as a housekeeping gene. The qPCR reaction solution consisted of 3μL cDNA, 5μL 2×Universal Blue SYBR Green qPCR Master Mix, and 2μL primers (1μL forward primer and 1μL reverse primer). The amplification conditions were 95°C for 1 min, followed by 40 cycles of 95°C for 20s, 55°C for 20s, and 72°C for 30s. The results were analyzed using the $2^{-\Delta\Delta}$Ct.

Statistical Analysis

The age was compared by Mann–Whitney *U*-test. The gender is compared by chi-squared test. All microarray data were standardized using the R package (version 4.2.1). Differential lncRNAs and mRNAs were screened by independent samples *t*-test. The linear regression analysis and Spearman's rank correlation test were used to verify the interaction role of lncRNA-mRNA in ceRNA network. MedCalc 15.2.0 software was used to draw the receiver operating characteristic (ROC) curves. The area under the curve (AUC) from ROC analysis was used to evaluate the diagnostic performance. P value less than 0.05 was considered to be statistically significant. The heatmaps, volcano graphs and venn diagram were drawn by online software.

Results

Patients' Characteristics

The demographic features between the two groups were summarized in Table 1. There were no significant differences in smoking history (p = 0.500), hypertension (p = 0.222), and diabetes (p = 0.222) between the TAAD group and ischemic heart group. The RBC (p = 0.008) and Hb (p = 0.008) in the TAAD groups were significantly lower than in ischemic heart group, respectively. The WBC was higher in patients with TAAD, but there was no significant difference ($9*10^9$/L vs $5.6*10^9$/L, p = 0.056). The patients in the TAAD group had significantly higher NEUT [7.73 (6.03, 9.98) $*10^9$/L] compared with those in ischemic heart group [4.06 (3.06, 5.09) mg/L, p = 0.016]. In addition, the level of CK in TAAD was higher than in ischemic heart group [546.80 (481.95, 920.75) vs 200.90 (157.95, 255.10) IU/L, p = 0.008] (Table 1).

Identification of Differentially Expressed Genes in Aortic Dissection

We compared the genes between TAAD and control group with our microarray dataset, and 95 DElncRNAs were found to be up-regulated and 66 down-regulated in TAAD. Alao, 54 DEmRNAs were up-regulated and 49 were down-regulated in TAAD (Supplemental Tables 1 and 2). The heatmaps and volcano plots of DEGs are shown in Figure 1A–D, respectively. According to the cut-off criterion, differentially expressed miRNAs (33 up-regulated and 54 down-regulated) were obtained from GSE98770 (Figure 1E and F).

GO Functional Enrichment Analysis of Up-DEGs and Down-DEGs in TAAD

To explore the functions enrichment pathways of these DEGs, GO and KEGG analyses were performed on up-DEGs and down-DEGs, respectively. As for GO analysis, we analyzed three subontologies of DEGs: cellular components (CC), molecular functions (MF), and biological processes (BP) (Figure 2).

The cellular component of up-DEGs were mainly enriched in lysosomal lumen, endosome lumen, vacuolar lumen, endolysosome, and collagen-containing extracellular matrix. The molecular function of up-DEGs were mainly enriched

Table 1 The Demographic, Clinical, and Laboratory Features Between the TAAD and the Ischemic Heart Disease Group

	Stanford-A Aortic Dissection (n=5)	Ischemic Heart Disease (n=5)	P Value
Demographic parameters			
Age (years)	57.00 (52.50, 61.00)	58.00 (58.00, 60.50)	0.421
Male/Female, n	4 / 1	5 / 0	1.000
Smoker, n(%)	3 (60%)	2 (40%)	0.500
Hypertension (%)	2 (40%)	3 (60%)	0.500
Diabetes (%)	0	2 (40%)	0.222
Laboratory parameters			
WBC ($*10^9$/L)	9.00 (7.35, 12.00)	5.60 (5.30, 8.05)	0.056
RBC ($*10^{12}$/L)	3.70 (3.44, 3.94)	4.50 (4.34, 4.84)	0.008
Hb (g/L)	113.00 (103.00, 122.50)	140.00 (132.50, 151.00)	0.008
PLT ($*10^9$/L)	124.00 (98.00, 208.00)	189.00 (166.00, 289.50)	0.222
LYMPH ($*10^9$/L)	0.56 (0.42, 1.20)	1.47 (1.17, 2.22)	0.032
MONO ($*10^9$/L)	1.02 (0.43, 1.27)	0.41 (0.34, 0.53)	0.151
NEUT ($*10^9$/L)	7.73 (6.03, 9.98)	4.06 (3.06, 5.09)	0.016
EO ($*10^9$/L)	0.00 (0.00, 0.01)	0.14 (0.07, 0.23)	0.008
BASO ($*10^9$/L)	0.01 (0.01, 0.02)	0.03 (0.03, 0.05)	0.008
Cr (μmol/L)	85.90 (72.85, 93.15)	86.40 (75.70, 139.20)	0.690
CK (IU/L)	546.80 (481.95, 920.75)	200.90 (157.95, 255.10)	0.008

Notes: The age is reported as the medians (IQR) and compared by Mann–Whitney *U*-test. The gender is reported as numbers and compared by chi-squared.

Abbreviations: WBC, white blood cell; RBC, red blood cell; Hb, hemoglobin; PLT, platelet count; LYMPH, lymphocyte; MONO, monocyte; NEUT, neutrophile; EO, eosinophil; BASO, basophil; Cr, creatinine; CK, creatine kinase.

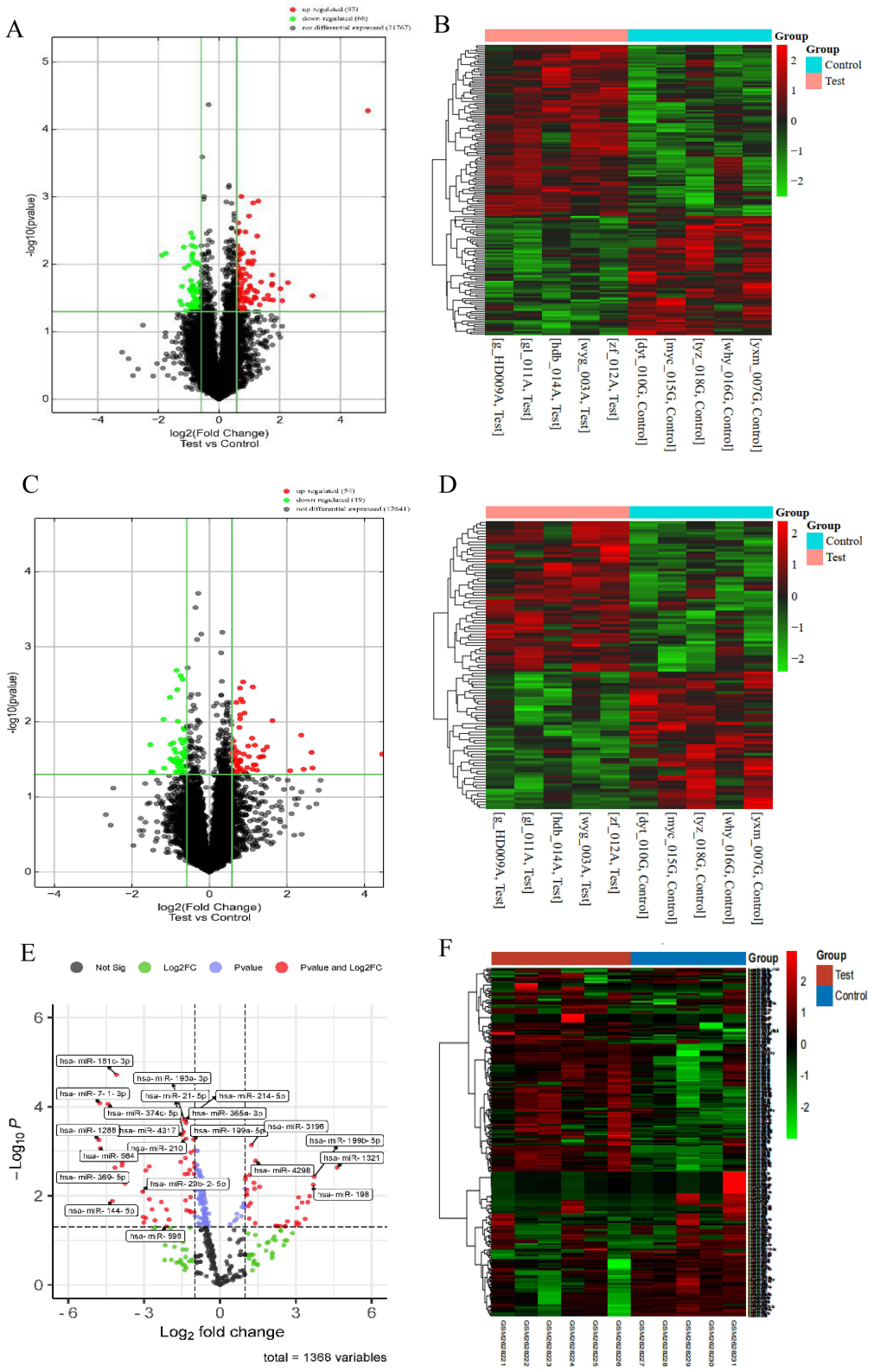

Figure 1 Differentially expressed analysis of lncRNAs, miRNAs and mRNAs. (**A** and **B**) The volcano map and heatmap of lncRNA expression profile in microarray dataset. (**C** and **D**) The volcano map and heatmap of mRNA expression profile in microarray dataset. (**E** and **F**) The volcano map and heatmap of miRNAs in GSE98770. In the volcano graph, the X-axis represents the fold changes of differently expressed mRNAs, and the Y-axis represents the adjusted p-value, red dots present up-regulated genes and blue dots present down-regulated genes (|log2foldChange| >1.0 and adjusted P value <0.05).

https://doi.org/10.2147/IJGM.S509177

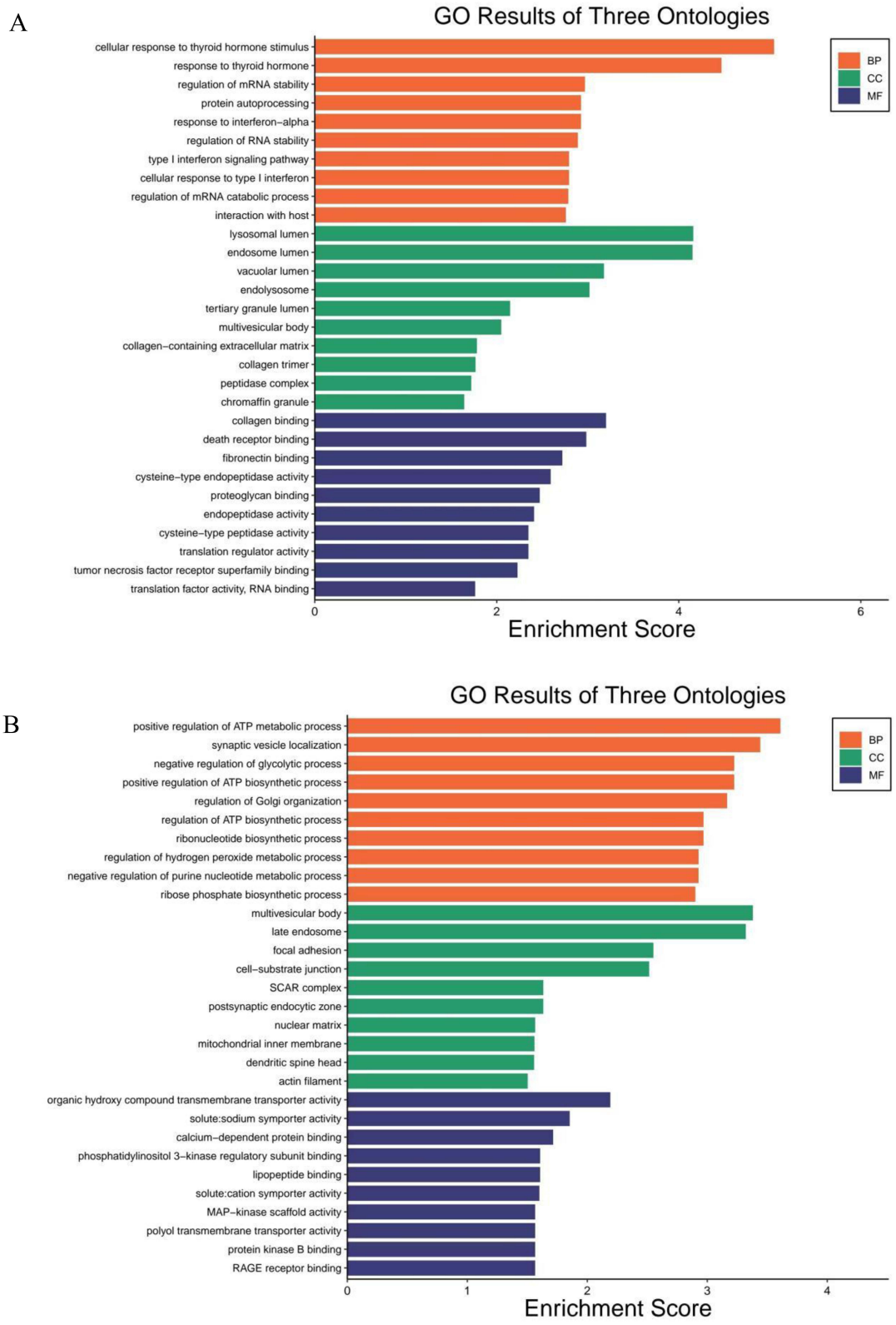

Figure 2 GO functional enrichment analysis of differentially expressed genes in AD. (**A**) GO analysis of down-regulated genes, including the top 10 biological processes, cellular component, and molecular function. (**B**) GO analysis of down-regulated genes, including the top 10 biological processes, cellular component, and molecular function. Red indicated biological processes; green indicated cellular component; blue indicated molecular function.

in fibronectin binding, death receptor binding, collagen binding, proteoglycan binding, and cysteine-type endopeptidase activity. The biological processes of up-DEGs were mainly enriched in cellular response to thyroid hormone stimulus, regulation of mRNA stability, regulation of mRNA catabolic process, response to thyroid hormone, and regulation of RNA stability (Supplemental Table 3).

As shown in Supplemental Table 4, the cellular component of down-DEGs were mainly focused on multivesicular body, late endosome, focal adhesion, cell substrate junction, SCAR complex, and actin filament. The molecular function of down-DEGs were mainly enriched in organic hydroxy compound transmembrane, transporter activity, solute:sodium symporter activity, calcium-dependent protein binding, and phosphatidylinositol 3-kinase regulatory subunit binding. The biological processes of down-DEGs were mainly enriched in positive regulation of ATP metabolic process, positive regulation of ATP biosynthetic process, regulation of ATP biosynthetic process, ribonucleotide biosynthetic process, and ribose phosphate biosynthetic process.

KEGG Signaling Pathway Analysis of Up-DEGs and Down-DEGs in TAAD

The KEGG analysis of up-DEGs and down-DEGs in TAAD were summarized in Supplemental Table 5. The pathway enrichment analysis revealed that up-regulated genes were mainly enriched in lysosome, apoptosis, phagosome, antigen processing and presentation, and sulfur metabolism (Figure 3A). The down-regulated genes were mainly focused on Salmonella infection, phospholipase D signaling pathway, acute myeloid leukemia, prolactin signaling pathway, and non-small cell lung cancer (Figure 3B). PIDD1 plays a major role in apoptosis pathway, GM2A plays a major role in lysosomal pathway, and CTSL, Cathepsin S (CTSS) and CTSH participate in both pathways (Figure 3C). The main genes enriched in Salmonella infection pathway are NCKAP1, DNM2, MAP2K2, CYTH1, and FLNB (Figure 3D).

PPI Network Construction and Identification of Hub Genes

The DEGs was imported into the STRING database and the PPI network was constructed. Cytohubba analysis was performed on the PPI data using Cytoscape to obtain the central gene. In terms of medium-degree calculations, the top 10 pivotal genes were RNASEL, CTSL, LOX, CTSS, VCAN, PLOD2, IFITM2, CTSH, AMFR, and ZNRF4, among which RNASEL scored the highest (Figure 4A and B). The interaction scores between nodes in the STRING analysis were shown in Supplemental Table 6. GeneMANIA analysis of all central genes was performed. These central genes were mainly enriched in apoptosis (FDR: 9.33e-9, Coverage:9/164) and oxidative stress processes (FDR: 4.50e-8, Coverage: 5/14) (Figure 4C and D).

Target Gene Prediction by TargetScan and Candidate Gene Screening

TargetScan was used to predict the miRNAs that hub genes could bind to, and 87 miRNAs were obtained. To find miRNAs that were differentially expressed, the projected 87 miRNAs were contrasted with the differentially expressed miRNAs in the GSE98770 dataset, 7 miRNAs (hsa-miR-30c-5p, hsa-miR-30a-5p, hsa-miR-1271-5p, hsa-miR-186-5p, hsa-miR-23a-3p, hsa-miR-146a-5p, and hsa-miR-145-5p) were identified (Figure 5A). Furthermore, all lncRNAs predicted using the 7 miRNAs were compared to the differentially expressed lncRNAs in our microarray data. A venn diagram analysis revealed 7 lncRNAs that were differently expressed, includig LINC01122, SNHG16, TTN-AS1, LINC01355, HCG18, ALG1L9P, and THUMPD3-AS1. Among which, LINC01355 was the only gene upregulated (Figure 5B).

Construction of ceRNA Network

The lncRNA-miRNA-mRNA network was constructed using Cytoscape, including 2 lncRNA nodes, 7 mRNA nodes, 5 miRNA nodes and 28 edges (Figure 6A). The ceRNA acts as an endogenous sponge of miRNA, miRNA expression is opposite to lncRNA and mRNA. Based on the ceRNA theory, 1 up-regulated lncRNA (LINC01355), 4 down-regulated miRNAs (hsa-miR-30c-5p, hsa-miR-30a-5p, hsa-miR-186-5p, and hsa-miR-145-5p), and 7 up-regulated mRNAs (RNASEL, LOX, CTSS, VCAN, PLOD2, CTSH, and AMFR) were identified (Figure 6B).

Correlation Analysis of lncRNA and mRNA in ceRNA Network

To further confirmed the interaction between lncRNAs and mRNA, we obtained the aortic dissection gene expression data (GSE52093 and GSE190635) from the GEO database for correlation analysis. The results showed LINC01355 was positively correlated with VCAN, LOX, and CTSS in GSE52093 datasets (r=0.85, p=0.00042; r=0.68, p=0.015; r=0.67,

A

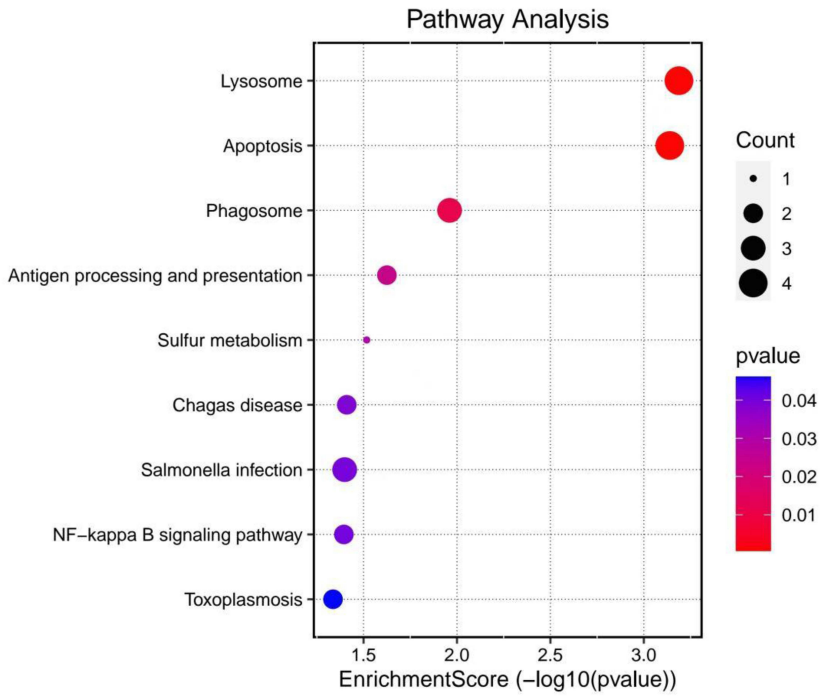

B

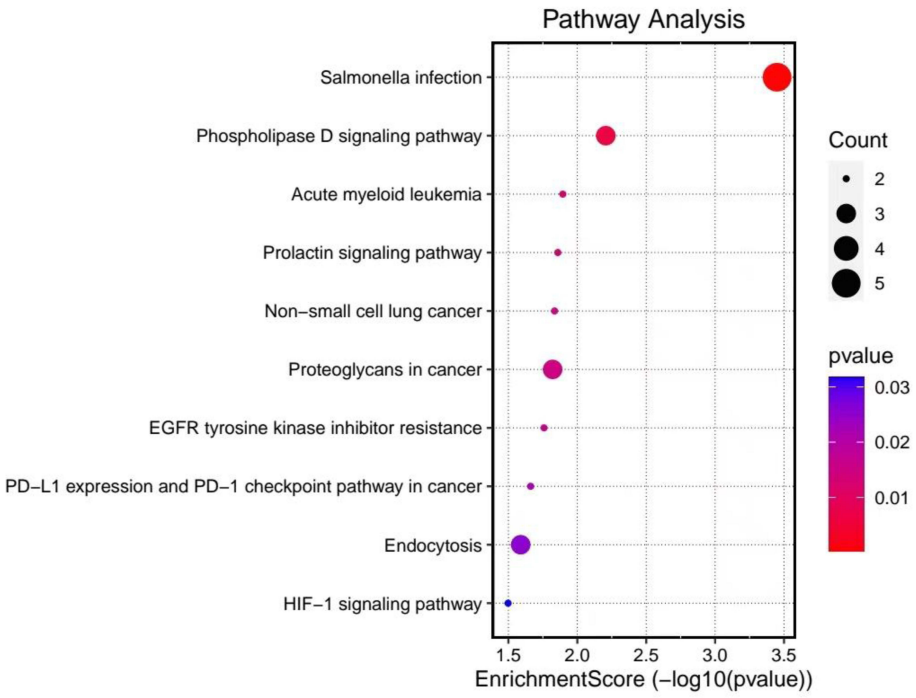

Figure 3 Continued.

(C)

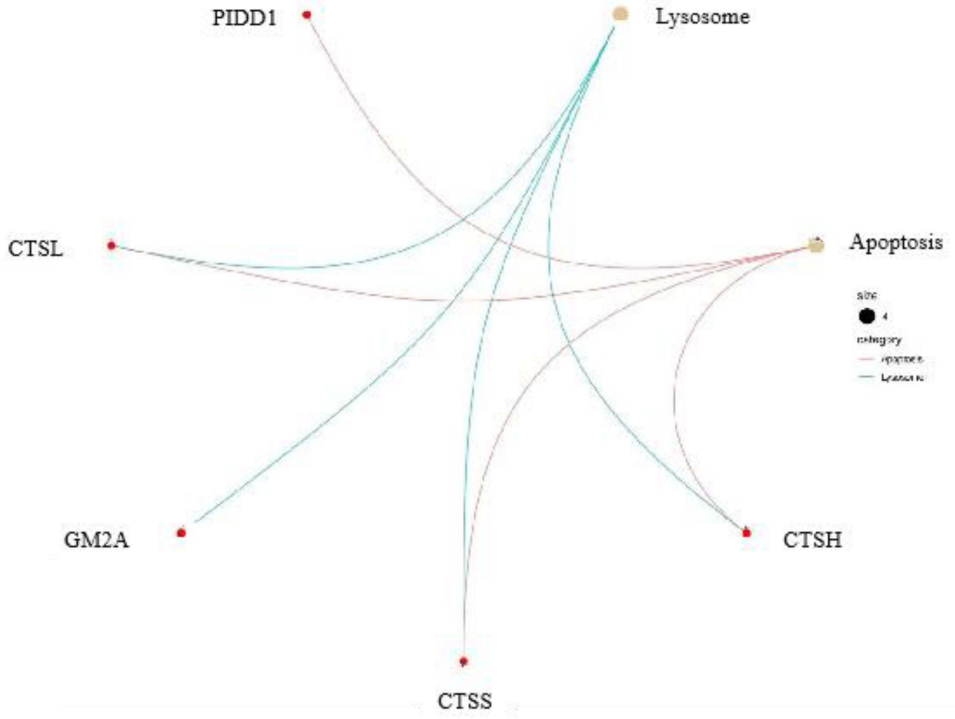

(D)

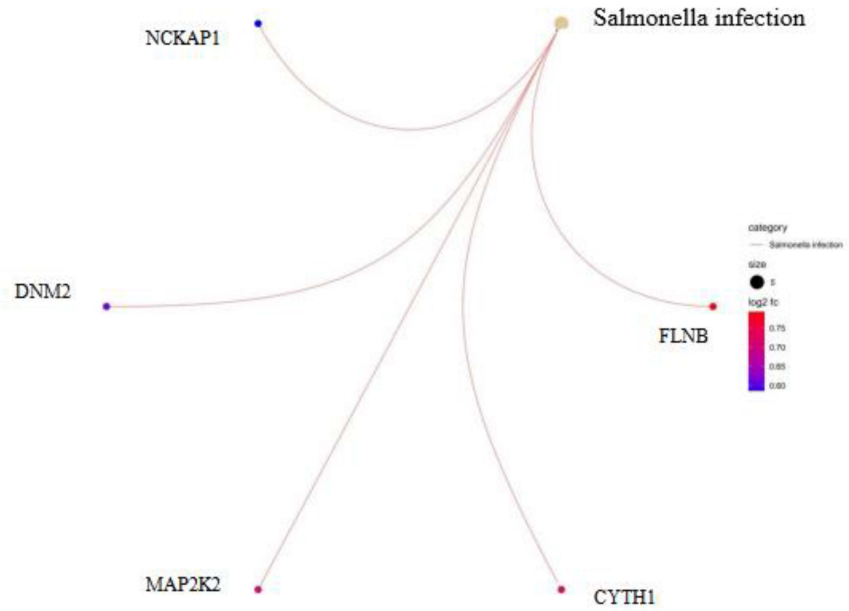

Figure 3 KEGG signaling pathway analysis of up-DEGs and down-DEGs in AD. (**A**) The top 5 signaling pathway analysis of up-regulated genes by KEGG. (**B**) The top 5 signaling pathway analysis of down-regulated genes by KEGG analysis. Gradual color means P value and the size means gene number. (**C**) Genes enriched in apoptosis and lysosomal pathways. Red lines indicated apoptosis pathway, blue lines indicated lysosome pathway. (**D**) Genes enriched in salmonella infection pathways.

https://doi.org/10.2147/IJGM.S509177

p=0.017, respectively; Figure 7A–C). In GSE190635 datasets, LINC01355 was also positively correlated with VCAN, LOX, and CTSS (r=0.85, p=0.0071; r=0.86, p=0.0057; r=0.90, p=0.0022, respectively; Figure 7D–F).

Clinical Performance of the VCAN, CTSS, and LOX for Diagnosing TAAD

The clinical performance of VCAN, CTSS, and LOX in terms of TAAD diagnosis was evaluated, and the results were summarized in Figure 8A. The AUCs of VCAN, CTSS, and LOX were 0.920 (95% confidence interval [CI] 0.580–0.999; p<0.001), 0.880 (95% CI 0.531–0.995; p=0.002) and 0.840 (95% CI 0.486–0.987; p=0.011), respectively. Furthermore, we conducted mRNA expression analysis in human aortic tissue. The results showed that VCAN

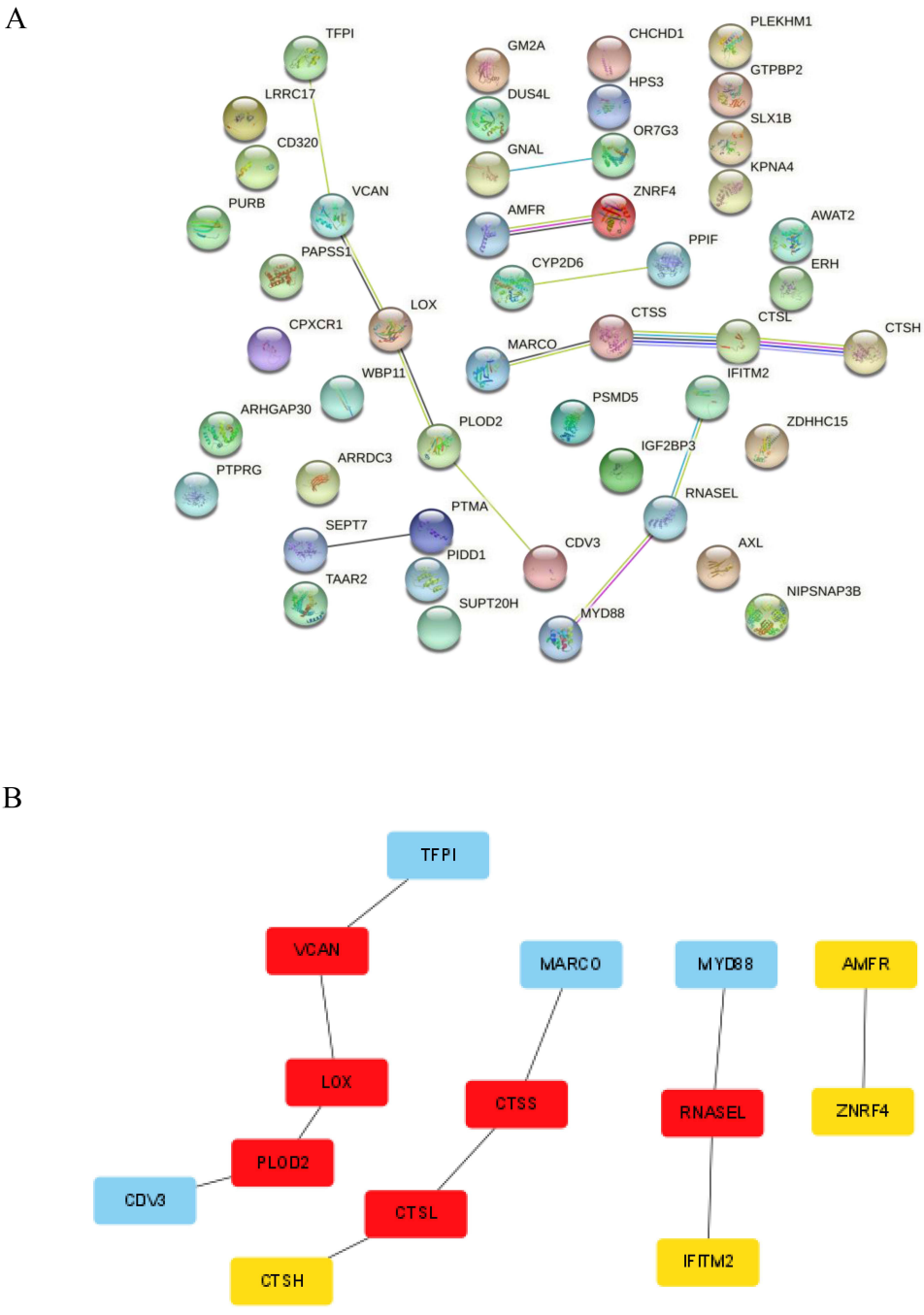

Figure 4 Continued.

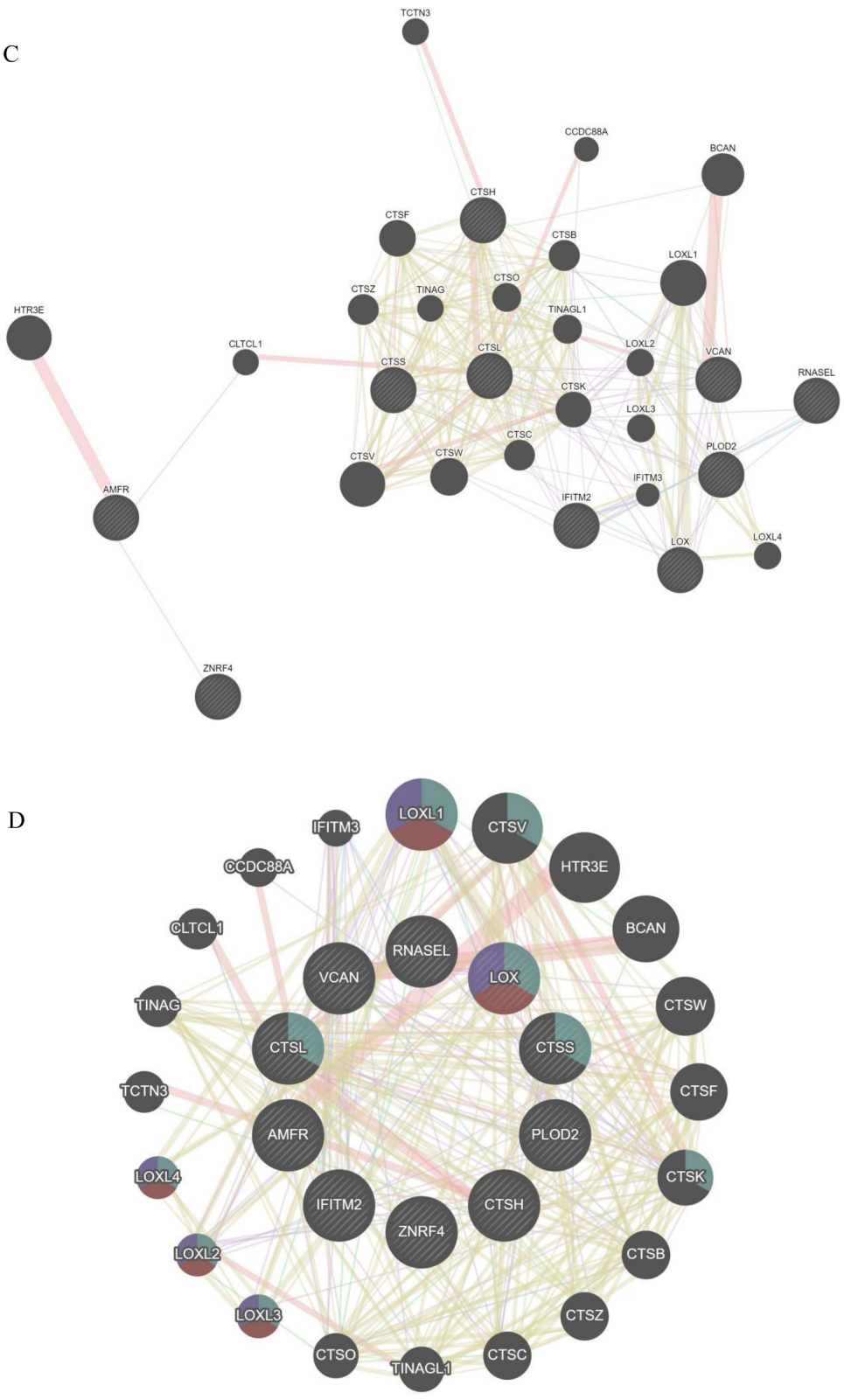

Figure 4 The interactome of DEGs by Cytoscape and hub genes by GeneMANIA analysis. (**A**) Protein-protein interaction networks of string database. (**B**) Cytohubba analysis predicts the hub genes by degree calculation. (**C**) Protein-protein interaction networks of the hub genes in apoptosis. (**D**) Enrich function of 10 hub genes in oxidative stress processes.

https://doi.org/10.2147/IJGM.S509177

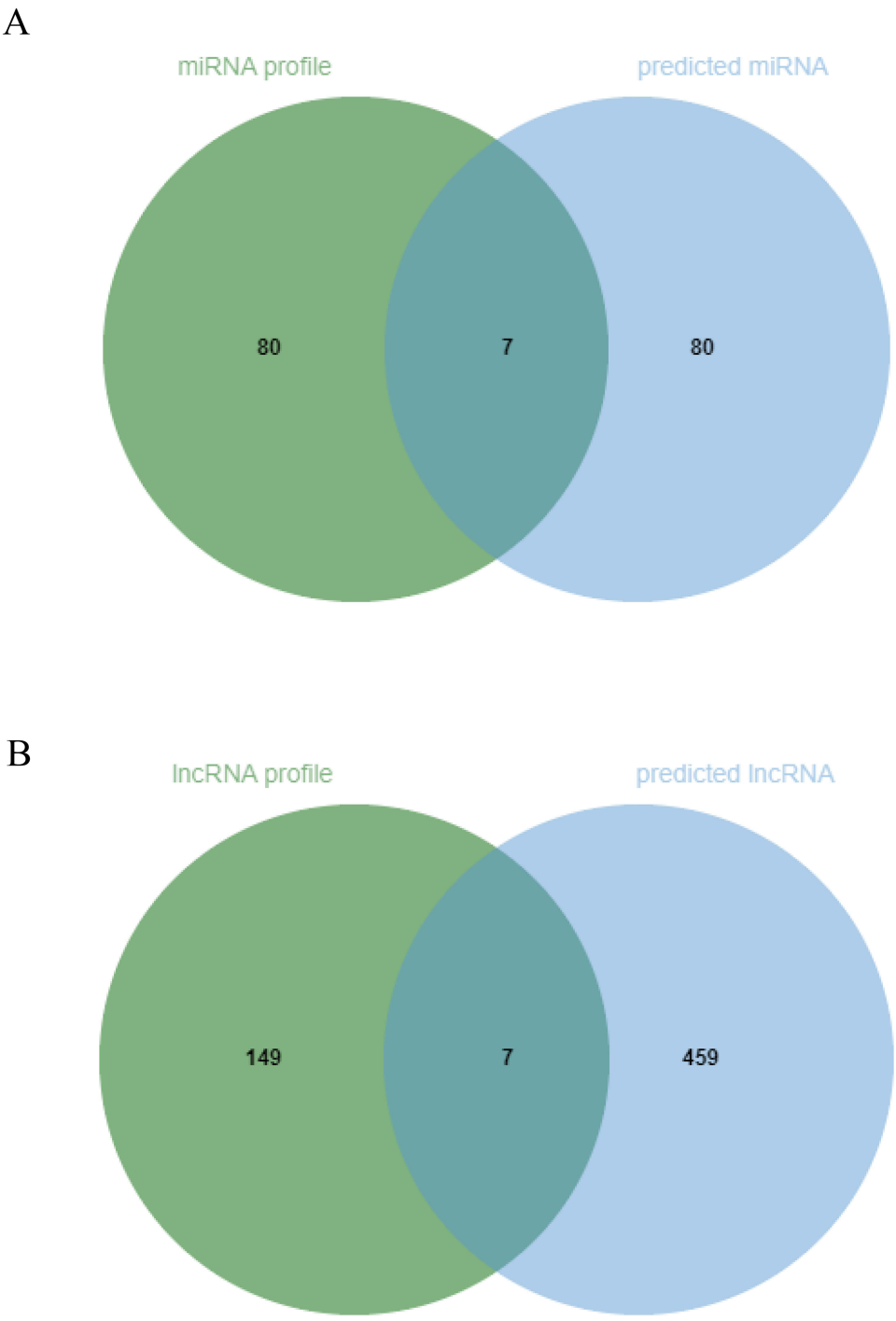

Figure 5 The candidate gene screening by predictive genes and microarray data. (**A**) The Venn diagram showed the differentially expressed miRNAs in the GSE98770 dataset and miRNA predicts by TargetScan online tool. (**B**) The differentially expressed lncRNAs in our microarray data and lncRNA predicts by TargetScan online tool. Blue indicated predicated miRNA/lncRNA, blue lines indicated miRNA/lncRNA in GSE98770 dataset/ microarray data.

($p<0.001$), CTSS ($p<0.001$), and LOX ($p=0.021$) significantly over-expressed in the TAAD patients, compared to control group (Figure 8B).

Discussion

TAAD is a rapidly progressing traumatic disease of the aorta with high morbidity and mortality.[11] Therefore, it is urgent to further explore the key molecular mechanisms of TAAD and find novel and specific biomarkers for early diagnosis and

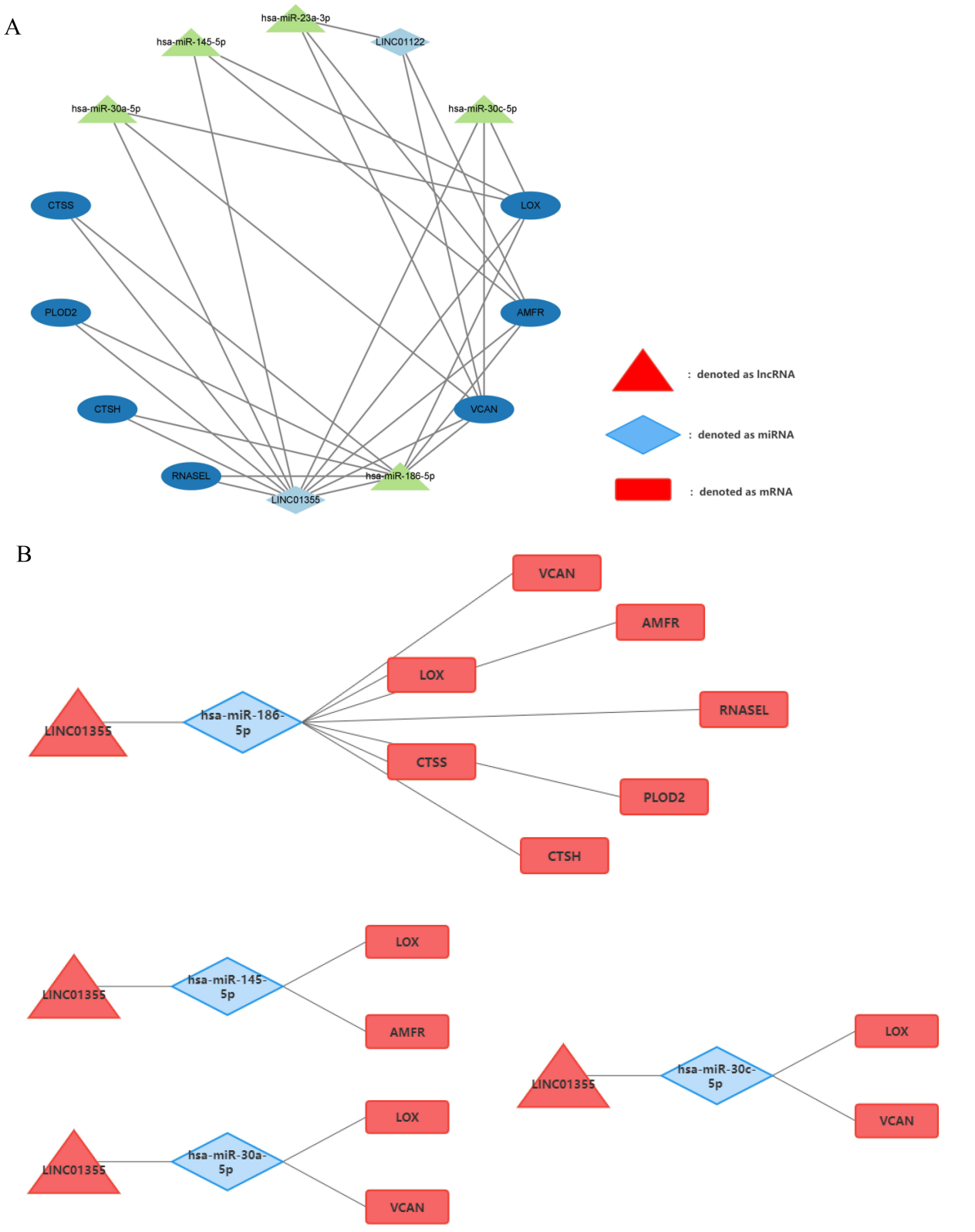

Figure 6 The CeRNA regulatory network by Cytoscape. (**A**) The CeRNA regulatory network, including the DElncRNA (LINC01355)-DEmiRNA (hsa-miR-30c-5p, hsa-miR-30a-5p, hsa-miR-186-5p, and hsa-miR-145-5p). (**B**) The CeRNA regulatory networks based on the hsa-miR-186-5p or hsa-miR-145-5p or hsa-miR-30c-5p or hsa-miR-30a-5p, respectively. Triangles, diamonds and rectangles indicated DElncRNAs, DEmiRNAs and DEmRNAs, respectively. Red and blue represented up- and down-regulation, respectively.

https://doi.org/10.2147/IJGM.S509177

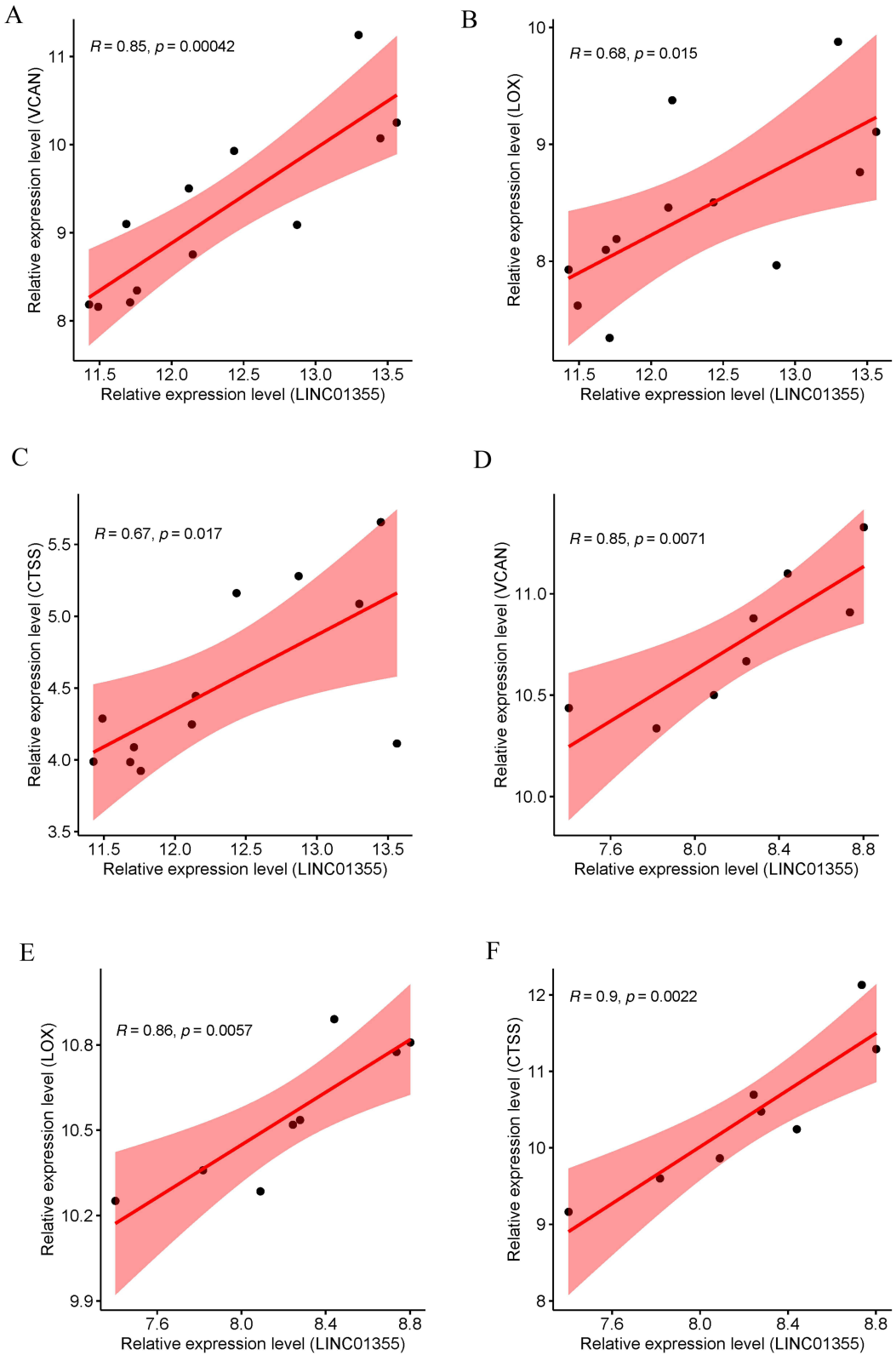

Figure 7 Correlation analysis of lncRNA and mRNA expression levels in ceRNA network. (**A-C**) The correlation between LINC01355 and VCAN, LOX, CTSS in GSE52093 datasets. (**D-F**) The correlation between LINC01355 and VCAN, LOX, CTSS in GSE190635 datasets.

(A)

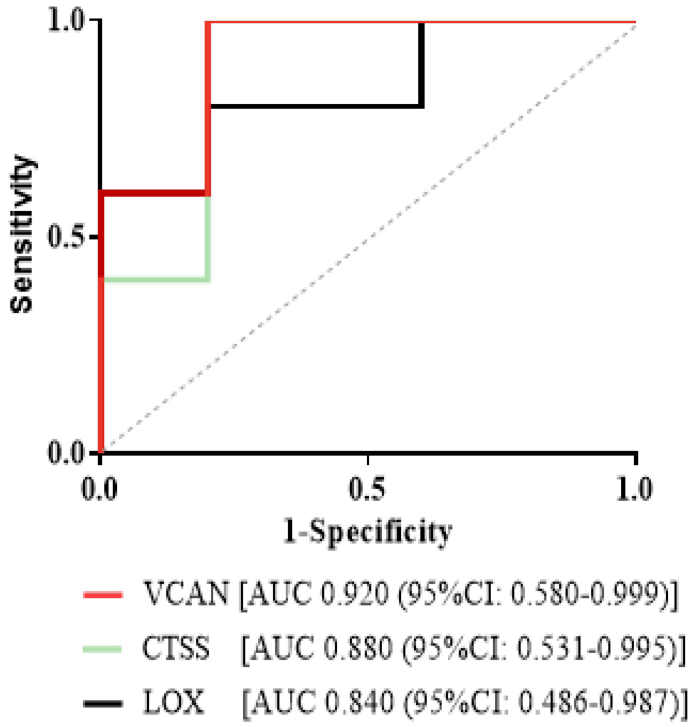

(B)

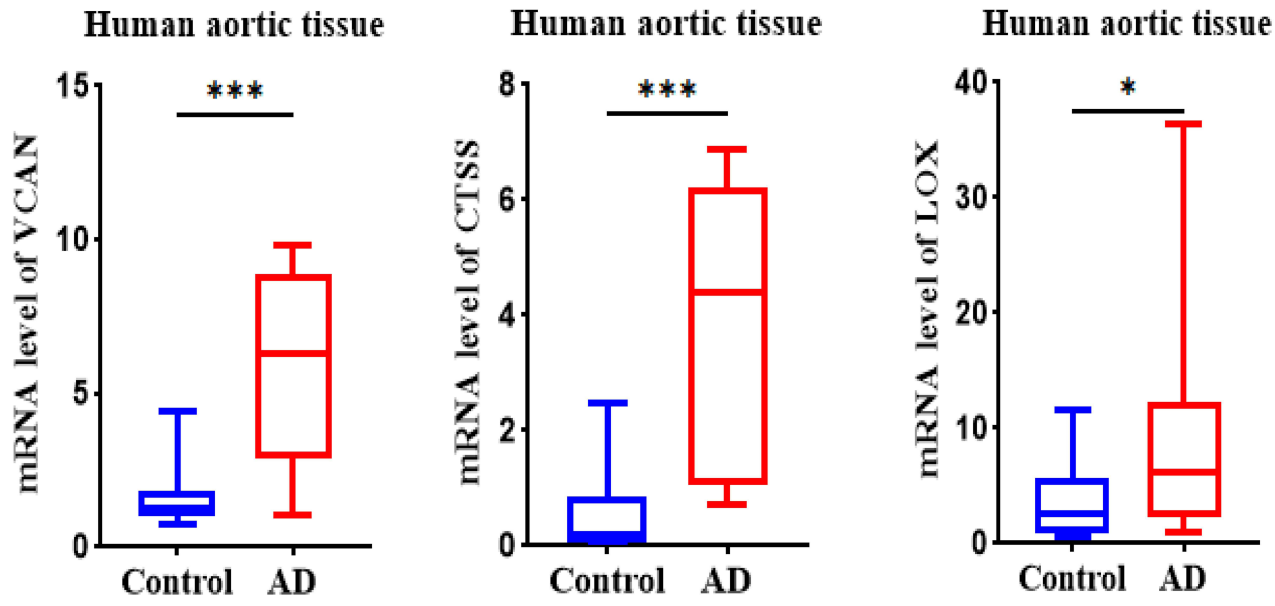

Figure 8 ROC analysis of VCAN, CTSS, and LOX for distinguishing patients with TAAD and controls and mRNA levels of VCAN in TAAD patients. (**A**) Red line indicated the AUC of VCAN; Green line indicated the AUC of CTSS; Black line indicated the AUC of LOX; dotted line indicated the AUC of MBC-IF assay. (**B**) The mRNA levels of VCAN, CTSS, and LOX between TAAD patients and control. * $p < 0.05$, *** $p < 0.001$.

https://doi.org/10.2147/IJGM.S509177

treatment. A growing number of studies suggest that differentially expressed RNAs, such as lncRNAs and miRNAs, may be a major cause of TAAD pathogenesis and progression.[12,13] To the best of our knowledge, previous bioinformatic analyses on TAAD and construction of ceRNA networks were from three databases of GEO (GSE 52093, GSE92427 and GSE98770), which undoubtedly has limitations.[14–16] To provide more possibilities for molecular studies of TAAD pathogenesis, lncRNA and mRNA expression profiles of TAAD and ischemic heart disease were obtained by microarray and high-throughput sequencing techniques in this study. Furthermore, bioinformatic analysis of the expression profile was performed to identify molecular networks important in the pathogenesis of TAAD, which may provide new guidance for the treatment of TAAD.

The microarray dataset showed that 103 DEmRNAs (54 up-regulated and 49 down-regulated) and 161 DElncRNAs (95 up-regulated and 66 down-regulated) were identified in aortic dissection samples, compared with normal ascending aortic samples. The up-DEGs by GO functional enrichment analysis showed that the up-regulated DEGs are mainly enriched in lysosomal lumen, endosome lumen, vacuolar lumen, endolysosome, and collagen-containing extracellular matrix and the down-DEGs are mainly enriched in multivesicular body, late endosome, focal adhesion, cell-substrate junction, SCAR complex, and actin filament. Up-regulated genes were primarily found in the lysosome pathway and the apoptotic pathway, according to KEGG analysis. Thus, GO and KEGG analysis revealed the importance of apoptosis in aortic mesangial vascular smooth muscle during TAAD. This conforms to the knowledge that vascular smooth muscle cell apoptosis is now thought to be a fundamental mechanism of TAAD development and progression. In addition to vascular smooth muscle cell apoptosis, the phenotypic transition of vascular smooth muscle cell plays a key role in triggering AD. Study demonstrated that vascular smooth muscle cell can reversibly switch from contractile to synthetic form in response to external stimulation, resulting in loss of contractile proteins and increase of inflammation, thereby accelerating aortic remodeling. Abhijit Chakraborty et al demonstrated that DNA damage and cytosolic leakage drive vascular smooth muscle cell from a contractile phenotype to an inflammatory phenotype.[17] Yongting Luo et al revealed that the TNF-OXPHOS-AP-1 axis triggers AD temporal-specific phenotypic transitions of vascular smooth muscle cell, leading to aortic dissection and rupture by single-cell RNA sequencing of human ascending aortas, validation experiments in human aortic tissues, primary human aortic vascular smooth muscle cell experiments, and a mouse model of AD.[18] However, the identified differential genes were not enriched for phenotypic transformation of vascular smooth muscle cells in our study.

Recently, an increasing number of studies have illustrated that lncRNA plays critical regulatory roles in cancer through lncRNA-miRNA-mRNA axes.[19] A sophisticated post-transcriptional endogenous regulatory network known as the ceRNA network has been proposed, in which lncRNAs and circRNAs serve as sponges for miRNAs to control mRNA, and miRNA expression is opposite to mRNAs.[20] The ceRNA network is involved in regulating proliferation, apoptosis, migration and phenotypic transformation of endothelial and smooth muscle cells in aortic dissection.[21,22] In this study, we constructed an TAAD-associated ceRNA network, including 2 lncRNA nodes, 7 mRNA nodes, and 5 miRNA nodes. Since ceRNA acts as a sponge for miRNAs, and lncRNAs in TAAD and control groups, we identified 1 up-regulated lncRNA (LINC01355), 4 down-regulated miRNAs (hsa-miR-30c-5p, hsa-miR-30a-5p, hsa-miR-186-5p, and hsa-miR-145-5p), and 7 up-regulated mRNAs (RNASEL, LOX, CTSS, VCAN, PLOD2, CTSH, and AMFR) based on the ceRNA theory. Bioinformatics analysis in this study indicated that the up-regulated DElncRNA (LINC01355) may compete with 4 key DEmiRNAs ((hsa-miR-30c-5p, hsa-miR-30a-5p, hsa-miR-186-5p, and hsa-miR-145-5p) to regulate the target DE mRNA expression of LINC01355, which is known as hypoxia yield proliferation associated lncRNA (HYPAL). According to research, LINC01355 accelerates the growth of gastric cancer cell via sponging miR-431-5p to activate CDK14.[23] Additionally, LINC01355 suppressed the growth of breast cancer by FOXO3-mediated transcriptional regulation of CCND1. Breast cancer cell proliferation was suppressed and cell cycle progression was arrested when LINC01355 was overexpressed.[24] This suggests that LINC01355 can act as a ceRNA to regulate cell proliferation apoptosis and cell cycle. Furthermore, it has been demonstrated that hsa-miR-186-5p, a component of the ceRNA network, is crucial in the rejection of cardiac transplants and mitigates propofol-induced cytotoxicity in cardiomyocytes produced from human induced pluripotent stem cells.[25,26] Also, it has been discovered that hsa-miR-186-5p participates in a new immune-associated ceRNA network.[27] Therefore, LINC01355 may compete as ceRNA for hsa-miR-186-5p to participate in regulating TAAD. Furthermore, logistic regression analysis confirmed that LINC01355 was positively correlated with VCAN, LOX, and CTSS in GSE52093 and GSE190635 datasets.

CTSS is thought to be a member of intra-lysosomal protein hydrolysis, degrading unwanted and damaged proteins.[28] It has been established that CTSS has a role in the extracellular matrix (ECM) protein degradation, protein trafficking, and cellular signaling during the pathophysiology of cardiovascular disease.[29] In atherosclerosis, for instance, CTSS is released into the ECM via lysosomal cytosolic action, enhancing collagen and elastin breakdown and encouraging VSMC migration.[30] Calcific aortic valve disease (CAVD) can cause degeneration and remodeling of the ECM, and CTSS is a key player.[31] It has also been shown that CTSS levels are increased in abdominal aortic aneurysms and are associated with HDL cholesterol and bilirubin.[32] Versican (VCAN), a vital extracellular matrix component, has an impact on inflammation through interactions with inflammatory cells, numerous cytokines and growth factors involved in the control of inflammation.[33] In addition, VCAN plays an important role in a variety of cancers and cardiovascular diseases as part of early inflammation.[34,35] It is worth noting that VCAN expression was found to be increased in thoracic aortic aneurysm and dissection (TAAD), suggesting a key role for proteoglycans in mediating medial aortic homeostasis and ECM integrity.[36] Based on the pathogenesis of inflammatory response, medial deformation, and loss of elastic fibers, it can be hypothesized that VCAN plays an important role in TAAD.[37,38] María Jesús Ruiz-Rodríguez et al demonstrated that VCAN plays a causative role in Marfan Syndrome (MFS) aortic disease in vivo by inducing Nos2 via Akt activation and identified components of the Akt signaling pathway as potential therapeutic targets.[39] Additionally, Frank S. Cikach et al has already elucidated and experimentally confirmed VCAN as a potential biomarker for aortic dissection.[36] These findings are to some extent consistent with the results of the present study. However, our study takes a different approach by integrating VCAN into a ceRNA (competing endogenous RNA) network. We identified novel regulatory relationships between VCAN and specific lncRNAs and miRNAs through bioinformatics analysis and subsequent experimental validation. Lysyl oxidase (LOX) and its related gene family members are involved in the two main structural proteins that build up the artery wall, elastin and collagen.[40] Current studies have shown that LOX loss-of-function mutations cause thoracic aortic aneurysms and coarctation in humans and may be a novel marker for TAAD with sensitivity and specificity comparable to that of TnT.[41,42] However, no studies have identified the upstream genes of LOX and how they affect the development of aortic coarctation by regulating LOX expression. This study predicted for the first time that LOX can be regulated through the ceRNA network in TAAD. Therefore, CTSS, VCAN, and LOX would be regulated through LINC01355.

The present study is a combination of data information and biological priori information, which may provide strong evidence for further investigation of the molecular mechanisms of TAAD. However, this study has a limitation due to the lack of correct for batch effects. The ComBat algorithm (from the R package sva) is a well-established and widely used method for adjusting batch effects in high-throughput genomic data. It could take into account the differences in sequencing platforms, sample processing methods, and other technical variability between datasets. This process minimize the technical variations between data sources and ensure that the subsequent data are more reliable. In the following studies, we will further verify the clear role of ceRNA network in the occurrence and development of TAAD, providing new therapeutic targets for TAAD.

Conclusion

In summary, the differential expression profile of lncRNA, miRNAs and mRNAs of TAAD in aortic dissection and the lncRNA-miRNA-mRNA regulatory axis were constructed by bioinformatics analysis. LOX axis, CTSS axis and VCAN axis may play important roles in TAAD. Our findings shed more light on the possible pathogenic mechanisms in TAAD using lncRNA-related ceRNA networks.

Data Sharing Statement

The data that support the findings of this study are available from the corresponding author, without undue reservation.

Ethical Approval and Consent to Participate

All patients provided the written informed consent. This study was approved by the Ethics Committee of Shanxi Medical University (SBQKL-2022-034) and was performed in accordance with the ethical standards in the 1964 Declaration of Helsinki.

Author Contributions

All authors made a significant contribution to the work reported, whether that is in the conception, study design, execution, acquisition of data, analysis and interpretation, or in all these areas; took part in drafting, revising or critically reviewing the article; gave final approval of the version to be published; have agreed on the journal to which the article has been submitted; and agree to be accountable for all aspects of the work.

Funding

This research was supported by the General Program of Natural Science Research of Science and Technology Department of Shanxi Province (No. 202203021211076), Fund Program for the Scientific Activities of Selected Returned Overseas Professionals in Shanxi Province (No. 2019-29) and Science and Technology Department of Shanxi Province (No. 201901D111403).

Disclosure

The authors declare that the research was conducted in the absence of any commercial or financial relationships.

References

1. Shah A, Khoynezhad A. Thoracic endovascular repair for acute type A aortic dissection: operative technique. *Ann Cardiothorac Surg*. 2016;5:389–396. doi:10.21037/acs.2016.07.08
2. Gudbjartsson T, Ahlsson A, Geirsson A, et al. Acute type A aortic dissection - a review. *Scand Cardiovasc J*. 2020;54:1–13. doi:10.1080/14017431.2019.1660401
3. Erbel R, Aboyans V, Boileau C, et al. 2014 ESC guidelines on the diagnosis and treatment of aortic diseases: document covering acute and chronic aortic diseases of the thoracic and abdominal aorta of the adult. The task force for the diagnosis and treatment of aortic diseases of the European Society of Cardiology (ESC). *Eur Heart J*. 2014;3:2873–2926. doi:10.1093/eurheartj/ehu281
4. Sun J, Chen G, Jing Y, et al. LncRNA expression profile of human thoracic aortic dissection by high-throughput sequencing. *Cell Physiol Biochem*. 2018;46:1027–1041. doi:10.1159/000488834
5. Wang W, Wang T, Wang Y, et al. Integration of gene expression profile data to verify hub genes of patients with Stanford A aortic dissection. *Biomed Res Int*. 2019;2019:3629751. doi:10.1155/2019/3629751
6. Batista PJ, Chang HY. Long noncoding RNAs: cellular address codes in development and disease. *Cell*. 2013;152:1298–1307. doi:10.1016/j.cell.2013.02.012
7. Ballantyne MD, McDonald RA, Baker AH. lncRNA/MicroRNA interactions in the vasculature. *Clin Pharmacol Ther*. 2016;99:494–501. doi:10.1002/cpt.355
8. Shen S, Jiang H, Bei Y, et al. Long non-coding RNAs in cardiac remodeling. *Cell Physiol Biochem*. 2017;41:1830–1837. doi:10.1159/000471913
9. Hu YY, Cheng XM, Wu N, et al. Non-coding RNAs regulate the pathogenesis of aortic dissection. *Front Cardiovasc Med*. 2022;9:890607. doi:10.3389/fcvm.2022.890607
10. Huang DW, Sherman BT, Tan Q, et al. The DAVID gene functional classification tool: a novel biological module-centric algorithm to functionally analyze large gene lists. *Genome Biol*. 2007;8:R183. doi:10.1186/gb-2007-8-9-r183
11. Levy D, Goyal A, Grigorova Y, et al. Aortic Dissection. In: *StatPearls*. Treasure Island (FL): StatPearls Publishing LLC.; 2022.
12. Kumar S, Boon RA, Maegdefessel L, et al. Role of noncoding RNAs in the pathogenesis of abdominal aortic aneurysm. *Circ Res*. 2019;124:619–630. doi:10.1161/CIRCRESAHA.118.312438
13. Cheng M, Yang Y, Xin H, et al. Non-coding RNAs in aortic dissection: from biomarkers to therapeutic targets. *J Cell Mol Med*. 2020;24:11622–11637. doi:10.1111/jcmm.15802
14. Zhang H, Bian C, Tu S, et al. Integrated analysis of lncRNA-miRNA-mRNA ceRNA network in human aortic dissection. *BMC Genomics*. 2021;22:724. doi:10.1186/s12864-021-08012-3
15. Shao Y, Luo J, Ye L, et al. Construction and integrated analysis of competitive endogenous long non-coding RNA network in thoracic aortic dissection. *Int J Gen Med*. 2021;14:6863–6873. doi:10.2147/IJGM.S335082
16. Gao H, Sun X, Liu Y, et al. Analysis of hub genes and the mechanism of immune infiltration in Stanford Type a Aortic Dissection. *Front Cardiovasc Med*. 2021;8:680065. doi:10.3389/fcvm.2021.680065
17. Chakraborty A, Li Y, Zhang C, et al. Epigenetic induction of smooth muscle cell phenotypic alterations in aortic aneurysms and dissections. *Circulation*. 2023;148:959–977. doi:10.1161/CIRCULATIONAHA.123.063332
18. Luo Y, Luo J, An P, et al. The activator protein-1 complex governs a vascular degenerative transcriptional programme in smooth muscle cells to trigger aortic dissection and rupture. *Eur Heart J*. 2024;45:287–305. doi:10.1093/eurheartj/ehad534
19. Zhang Q, Sun L, Zhang Q, et al. Construction of a disease-specific lncRNA-miRNA-mRNA regulatory network reveals potential regulatory axes and prognostic biomarkers for hepatocellular carcinoma. *Cancer Med*. 2020;9:9219–9235. doi:10.1002/cam4.3526
20. Chen YH, Zhong LF, Hong X, et al. Integrated analysis of circRNA-miRNA-mRNA ceRNA network in cardiac hypertrophy. *Front Genet*. 2022;13:781676. doi:10.3389/fgene.2022.781676
21. Zhang S, Zhao S, Han X, et al. Lnc-C2orf63-4-1 Confers VSMC homeostasis and prevents aortic dissection formation via STAT3 interaction. *Front Cell Dev Biol*. 2021;9:792051. doi:10.3389/fcell.2021.792051
22. Xu Z, Zhong K, Guo G, et al. circ_TGFBR2 inhibits vascular smooth muscle cells phenotypic switch and suppresses aortic dissection progression by sponging miR-29a. *J Inflamm Res*. 2021;14:5877–5890. doi:10.2147/JIR.S336094

23. Piao HY, Liu Y, Kang Y, et al. Hypoxia associated lncRNA HYPAL promotes proliferation of gastric cancer as ceRNA by sponging miR-431-5p to upregulate CDK14. *Gastric Cancer*. 2022;25:44–63. doi:10.1007/s10120-021-01213-5
24. Ai B, Kong X, Wang X, et al. LINC01355 suppresses breast cancer growth through FOXO3-mediated transcriptional repression of CCND1. *Cell Death Dis*. 2019;10:502. doi:10.1038/s41419-019-1741-8
25. Ren Z, Hu R. Downregulation of long noncoding RNA SNHG6 rescued propofol-induced cytotoxicity in human induced pluripotent stem cell-derived cardiomyocytes. *Cardiovasc Diagn Ther*. 2020;10:811–819. doi:10.21037/cdt-20-443
26. Kennel PJ, Yahi A, Naka Y, et al. Longitudinal profiling of circulating miRNA during cardiac allograft rejection: a proof-of-concept study. *ESC Heart Fail*. 2021;8:1840–1849. doi:10.1002/ehf2.13238
27. Li W, Meng X, Yuan H, et al. A novel immune-related ceRNA network and relative potential therapeutic drug prediction in ccRCC. *Front Genet*. 2022;12:755706. doi:10.3389/fgene.2021.755706
28. Smyth P, Sasiwachirangkul J, Williams R, et al. Cathepsin S (CTSS) activity in health and disease - A treasure trove of untapped clinical potential. *mol Aspects Med*. 2022;88:101106. doi:10.1016/j.mam.2022.101106
29. Wu H, Du Q, Dai Q, et al. Cysteine protease cathepsins in atherosclerotic cardiovascular diseases. *J Atheroscler Thromb*. 2018;25:111–123. doi:10.5551/jat.RV17016
30. Ni H, Xu S, Chen H, et al. Nicotine modulates CTSS (cathepsin S) synthesis and secretion through regulating the autophagy-lysosomal machinery in atherosclerosis. *Arterioscler Thromb Vasc Biol*. 2020;40:2054–2069. doi:10.1161/ATVBAHA.120.314053
31. Sun L, Chandra S, Sucosky P. Ex vivo evidence for the contribution of hemodynamic shear stress abnormalities to the early pathogenesis of calcific bicuspid aortic valve disease. *PLoS One*. 2012;7:e48843. doi:10.1371/journal.pone.0048843
32. Mirjanic-Azaric B, Vasic N, Cerne D, et al. Plasma cathepsin S is associated with high-density lipoprotein cholesterol and bilirubin in patients with abdominal aortic aneurysms. *J Med Biochem*. 2019;38:268–275. doi:10.2478/jomb-2018-0039
33. Xu L, Xue T, Zhang J, et al. Knockdown of versican V1 induces a severe inflammatory response in LPS-induced acute lung injury via the TLR2-NF-κB signaling pathway in C57BL/6J mice. *Mol Med Rep*. 2016;13:5005–5012. doi:10.3892/mmr.2016.5168
34. Naboulsi W, Megger DA, Bracht T, et al. Quantitative tissue proteomics analysis reveals versican as potential biomarker for early-stage hepatocellular carcinoma. *J Proteome Res*. 2016;15:38–47. doi:10.1021/acs.jproteome.5b00420
35. Otsuka F, Kramer MC, Woudstra P, et al. Natural progression of atherosclerosis from pathologic intimal thickening to late fibroatheroma in human coronary arteries: a pathology study. *Atherosclerosis*. 2015;241:772–782. doi:10.1016/j.atherosclerosis.2015.05.011
36. Cikach FS, Koch CD, Mead TJ, et al. Massive aggrecan and versican accumulation in thoracic aortic aneurysm and dissection. *JCI Insight*. 2018;3:e97167. doi:10.1172/jci.insight.97167
37. Humphrey JD. Possible mechanical roles of glycosaminoglycans in thoracic aortic dissection and associations with dysregulated transforming growth factor-β. *J Vasc Res*. 2013;50:1–10. doi:10.1159/000342436
38. Gawinecka J, Schönrath F, von Eckardstein A. Acute aortic dissection: pathogenesis, risk factors and diagnosis. *Swiss Med Wkly*. 2017;147:w14489. doi:10.4414/smw.2017.14489
39. Ruiz-Rodríguez MJ, Oller J, Martínez-Martínez S, et al. Versican accumulation drives Nos2 induction and aortic disease in Marfan syndrome via Akt activation. *EMBO Mol Med*. 2024;16:132–157. doi:10.1038/s44321-023-00009-7
40. Yi X, Zhou Y, Chen Y, et al. The expression patterns and roles of lysyl oxidases in aortic dissection. *Front Cardiovasc Med*. 2021;8:692856. doi:10.3389/fcvm.2021.692856
41. Hofmann A, Brunssen C, Wolk S, et al. Soluble LOX-1: a novel biomarker in patients with coronary artery disease, stroke, and acute aortic dissection? *J Am Heart Assoc*. 2020;9:e013803. doi:10.1161/JAHA.119.013803
42. Chen Y, Zhang T, Yao F, et al. Dysregulation of interaction between LOXhigh fibroblast and smooth muscle cells contributes to the pathogenesis of aortic dissection. *Theranostics*. 2022;12:910–928. doi:10.7150/thno.66059